Biological Psychiatry: CNNI

Archival Report

Resting-State Changes in Aging and Parkinson's Disease Are Shaped by Underlying Neurotransmission: A Normative Modeling Study

Jan Kasper, Svenja Caspers, Leon D. Lotter, Felix Hoffstaedter, Simon B. Eickhoff, and Juergen Dukart

ABSTRACT

BACKGROUND: Human healthy and pathological aging is linked to a steady decline in brain resting-state activity and connectivity measures. The neurophysiological mechanisms that underlie these changes remain poorly understood.

METHODS: Making use of recent developments in normative modeling and availability of in vivo maps for various neurochemical systems, we tested in the UK Biobank cohort (n = 25,917) whether and how age- and Parkinson's disease–related resting-state changes in commonly applied local and global activity and connectivity measures colocalize with underlying neurotransmitter systems.

RESULTS: We found that the distributions of several major neurotransmitter systems including serotonergic, dopaminergic, noradrenergic, and glutamatergic neurotransmission correlated with age-related changes across functional activity and connectivity measures. Colocalization patterns in Parkinson's disease deviated from normative aging trajectories for these, as well as for cholinergic and GABAergic (gamma-aminobutyric acidergic) neurotransmission. The deviation from normal colocalization of brain function and $GABA_A$ correlated with disease duration.

CONCLUSIONS: These findings provide new insights into molecular mechanisms underlying age- and Parkinson's-related brain functional changes by extending the existing evidence elucidating the vulnerability of specific neurochemical attributes to normal aging and Parkinson's disease. The results particularly indicate that alongside dopamine and serotonin, increased vulnerability of glutamatergic, cholinergic, and GABAergic systems may also contribute to Parkinson's disease–related functional alterations. Combining normative modeling and neurotransmitter mapping may aid future research and drug development through deeper understanding of neurophysiological mechanisms that underlie specific clinical conditions.

https://doi.org/10.1016/j.bpsc.2024.04.010

Understanding neurophysiological mechanisms that underlie healthy and pathological brain aging is essential for successful prevention, detection, and intervention strategies against age-related diseases and cognitive decline. Despite ample evidence for age-related decline in various brain functional measures, understanding of the neurophysiological mechanisms that underlie these changes is limited. Because the interplay among different neurotransmitter systems contributes substantially to the blood oxygen level–dependent (BOLD) signal, changes in these systems likely contribute to age-related functional alterations as observed using resting-state functional magnetic resonance imaging (rs-fMRI).

Most commonly applied rs-fMRI measures estimate either local activity or synchronicity by assessing temporal changes in regional BOLD amplitude or BOLD signal correlation across regions. Previous rs-fMRI studies have reported aging-related reductions in local brain activity primarily in medial and frontal regions (1–4). These alterations are complemented by reduced local synchronicity in cortical, subcortical, and cerebellar motor structures (5) and increased local synchronicity mainly in hippocampal and thalamic regions (4,6). Positron emission tomography (PET) studies of aging have found reduced serotonergic (7–11), dopaminergic (12–15), glutamatergic (16–18), cholinergic (19), and norepinephrinergic (20) neurotransmission and increased availability of $GABA_A$ (gamma-aminobutyric acid A) (21) and μ opioid (22) receptors. While both modalities point to complex functional reorganization during aging, the relationship between the respective rs-fMRI and PET findings remains poorly understood.

Studying associations between PET-derived regional receptor or transporter availability and rs-fMRI–derived functional signal has been shown to be a promising way to estimate their impact on the observed brain phenotypes (23,24). However, age-related changes in these associations have not been systematically addressed. These changes may reflect altered availability or functional decline of cell populations with corresponding neurochemical properties. Following this logic, disease-related changes in such

SEE COMMENTARY ON PAGE 969

associations would support the notion of respective neurotransmitter systems being particularly affected by the respective neuropathology (25).

Understanding of typical age-related colocalization changes of brain function and neurotransmitter systems can inform the study of pathological deviations from such as is observed in Parkinson's disease (PD), for example (25). Normative models, as recently applied to MRI data (26–28), may prove suitable for characterizing such spatial colocalizations. Such models allow individual participants or patients to be compared with the typical trajectories derived from large representative populations by incorporating nonconstant percentiles of variation and variation within the cohort of interest (29).

Previous studies have provided evidence for increased vulnerability of specific neurotransmitter systems in PD including dopaminergic (30–35), serotonergic (36–38), glutamatergic (39,40), GABAergic (34), histaminergic (41), cholinergic (42–44), and norepinephrinergic (45,46) neurotransmission. In our previous work, functional alterations in PD were related to the availability of D_2 and serotonin 1B ($5\text{-}HT_{1B}$) receptors, supporting the notion of specific vulnerability of these neurotransmitter systems (25). However, whether and how far these PD-related alterations deviate from typical age-related colocalization changes remain to be shown.

To address these questions, we adopted a normative modeling approach to testing for aging effects on colocalizations between brain functional measures and underlying neurotransmission in the UK Biobank cohort. We tested for colocalization of PET-derived distributions for major neurotransmitter systems with commonly deployed rs-fMRI–derived activity and connectivity measures during aging and in PD.

METHODS AND MATERIALS

Cohorts

We included 25,917 adult participants from the UK Biobank not diagnosed with psychiatric, cognitive, or neurological disorders (Table S1) with known effects on brain structure and function as a control cohort. We also identified a group of 58 participants from the UK Biobank who were diagnosed with idiopathic PD (ICD-10, G20) before their imaging session. An overview of both groups is provided in Table 1.

Processing of Resting-State Functional Imaging Data

We used rs-fMRI data from the UK Biobank, initially processed according to their documentation (47). We normalized (Montreal Neurological Institute space), smoothed, and bandpass-filtered these images to enhance the signal-to-noise ratio of neuronal activity in the BOLD signal. Control measures were implemented to mitigate confounding effects of motion, white matter, and cerebrospinal fluid. Data quality was further improved by discarding images exhibiting distortions and artifacts, including those attributed to within-scanner motion. Details on preprocessing procedures, metrics calculation, and key figures for data analysis are provided in the Supplemental Methods.

Three complementary voxelwise maps of brain function, including measures of neuronal activity and synchronicity, were derived from individual, preprocessed rs-fMRI data. Fractional amplitude of low-frequency fluctuations (fALFF) (48) was computed as the power ratio of neuronal activity–related oscillations to the total detectable frequency range in the BOLD signal. Local correlation (LCOR) (49) and global correlation (GCOR) (50) characterized BOLD similarity, reflecting the voxel's correlation either with its local vicinity or with all other voxels, respectively.

Aging Effects and Sex Differences in fALFF, LCOR, and GCOR

Both voxelwise aging effects and sex differences were estimated by general linear modeling of (t statistic) contrast maps using a familywise error–corrected voxelwise threshold of $p < .05$ combined with a cluster-defining threshold of $k > 20$ including sex or age and total intracranial volume as covariates, respectively. Maps of annual changes in fALFF, LCOR, and GCOR were generated from voxelwise beta weights.

Spatial Colocalization of Brain Function and Neurotransmitter Systems and Effects of Aging in the Healthy Control Participant Group

We analyzed to what extent unthresholded group-level aging effects (maps of annual change) on fALFF, LCOR, and GCOR colocalized with specific neurotransmitter systems. Spearman correlation coefficients were derived using the default Neuromorphometrics atlas (119 regions), estimating the similarity of

Table 1. Demographic Characteristics of the Study Sample

	HC				
	Combined, n = 25,917	Females, n = 14,000	Males, n = 11,917	Manifest PD, n = 58	HC Matched to PD, n = 17,400
Age, Years	64.03 ± 7.5	63.5 ± 7.4	64.7 ± 7.6	68.6 ± 6.5	67.6 ± 6.0
Age statistics	–	$t_{25915} = -12.48$, $p < .0001$, Cohen's $d = -0.16$		$t_{57.32} = 1.15$, $p = .26$	
Sex, Male	11,917 (46%)	–		32 (55.2%)	8988 (51.7%)
Sex statistics	–	–		$\chi^2_1 = 0.29$, $p = .59$	
TIV, L	1.548 ± 0.152	1.467 ± 0.116	1.643 ± 0.133	–	–
TIV statistics	–	$t_{25915} = -113.0$, $p < .0001$, Cohen's $d = -1.42$		–	–

Values are presented as n, mean ± SD, or n (%). Normative modeling of colocalizations between brain function and neurotransmitter systems was based on the data of HCs. Regional differences in brain measures in patients with PD were calculated with respect to an age- and sex-matched subcohort of HCs.

HC, healthy control participant; PD, Parkinson's disease; TIV, total intracranial volume.

aging effects in fALFF, LCOR, and GCOR with 19 distinct neurotransmitter maps as included in the JuSpace toolbox (25). To approximate a normal distribution, correlation coefficients were Fisher's *z*-transformed. As shown in our previous study (51), the choice of atlas (with a comparable number of parcels) has a negligible effect on the observed colocalization patterns. This atlas was used because it provides a neuroanatomically plausible delineation of cortical and subcortical structures.

Included PET maps were derived from independent healthy volunteer populations and covered serotonergic receptors [5-HT_{1A} (52), 5-HT_{1B} (53), 5-HT_{2A} (52), 5-HT_4 (52), 5-HT_6 (11)], dopaminergic receptors [D_1 (54), D_2 (55)], histamine H_3 receptor (56), dopamine uptake (24), serotonin (SERT) (52), norepinephrine (20), vesicular acetylcholine (VAChT) (57) transporters, cholinergic receptors [M1 (58), $\alpha4\beta2$ (59)], glutamate receptors [mGluR5 (60), NMDA (61)], and cannabinoid CB_1 (62), opioid μ (57), and the $GABA_A$ (24) receptor. Source publications and sample characteristics of each PET map are provided in Table S2. Ninety-five percent confidence intervals of Spearman correlation coefficients were estimated using the Bonett-Wright (63) procedure.

We recomputed correlations with all PET maps using single-participant measures of fALFF, LCOR, and GCOR for greater insight into how group-level aging effects are also reflected in the magnitude and spread across individual data. Before testing for aging effects across individual colocalizations, we examined whether Fisher's *z*-transformed Spearman correlation coefficients of the healthy population differed significantly from a null distribution (1-sample *t* test, alpha = 0.05). Aging effects on colocalization strengths were then estimated using linear regression analyses considering sex as a confound.

Higher Variation in Colocalization Between Brain Function and Neurotransmitter Systems With Aging

Distinct aging trajectories from healthy aging to the effects of diseases and impairments are known to manifest in altered brain function. Depending on the underlying neurophysiological processes, functional changes are likely to be architecturally aligned with the spatial patterns of affected neurotransmitter systems. Correspondingly, one would expect to observe increased variance in colocalizations in older than in younger participants. To test this hypothesis, we examined the heteroscedasticity to identify neurotransmitter systems affected by such age-related brain functional changes in 2 steps.

Using the White test, we first identified all pairs of brain function measures and PET maps whose correlation coefficients exhibited nonconstant variance across age. In a post hoc analysis, we tested for each colocalization pair with nonconstant variance (false discovery rate (FDR)–corrected *p* [p_{FDR}] $< .05$) whether the variance for individuals in the upper third age-range was higher than that for individuals in the lower third age range using the Goldfeld-Quandt-test (1-sided, i.e., increasing variance). We regressed out sex effects prior to the comparisons.

Normative Modeling of Brain Function: Neurotransmitter Colocalization and Deviations in PD

To model aging effects on the observed colocalization patterns, we generated normative models based on the Fisher's transformed correlation coefficients derived from the healthy participants using the PCNtoolkit (64) (cf. Supplemental Methods for more details on model construction and Figure 1 for a methodological overview).

For participants with PD, deviations (*z* scores) from these normative aging models were derived per neurotransmitter map. For each model, we examined whether the PD deviation scores were significantly different from a null distribution (*t* test, alpha = 0.05) and whether they were correlated with disease duration and cognitive scores (details are provided in Tables S23–S29). We also wanted to know which brain regions contributed most to significant deviations ($p_{FDR} < .05$) and whether functional differences from a normal subpopulation explain these regional contributions. To this end, we repeated the colocalization analysis in the data of the PD group using a leave-one-region-out approach (65) to obtain maps of regional contribution ($\Delta\rho^2$) to the deviation. Furthermore, we calculated regional functional differences (Cohen's *d*) in fALFF, LCOR, and GCOR in PD compared with an age- and sex-matched healthy subgroup (n = 17,400).

All analyses were corrected for multiple comparisons using either the Benjamini-Hochberg procedure or, in case of inflated *p* values due to large sample sizes, the Bonferroni-Holm correction. Additionally, to minimize the influence of underlying atrophy on colocalization changes, we repeated all analyses after regressing out individual voxelwise gray matter volumes from all functional maps.

RESULTS

Demographic Characteristics

From a total pool of 30,035 participants from the UK Biobank for whom all necessary data were available, our analysis was based on data of 25,917 participants for whom no diseases with known effect on brain function were reported.

The analysis was repeated on 25,914 participants after accounting for age-related atrophy, excluding 3 participants with structural data. Seventy-five participants in the total pool had reported a diagnosis of PD; 58 of them were classified as "manifest" because their first report of PD was dated before their imaging session. To compare regional measures of brain function in patients with PD with those of the healthy control participants (HCs), we defined an age- and sex-matched subcohort consisting of 17,400 participants (mean ± SD age in years: PD = 68.6 ± 6.5, HC = 67.6 ± 6.0, $p > .26$; PD 55.17% male and HC 51.7% male, $\chi^2_1 = 0.29$, $p = .59$). An overview of the groups is provided in Table 1.

Group-Level Aging Effects in Resting-State Measures and Their Colocalization to Underlying Neurotransmission

All 3 functional measures decreased with aging in most cortical, subcortical, and cerebellar regions. Each measure showed a widespread but distinct spatial pattern of age-related alterations with few regional increases (Figure 2A; Tables S3 and S4).

Next, we aimed to understand whether the topography of age-related changes was correlated with distributions of specific neurotransmitter systems. For this, we derived voxelwise

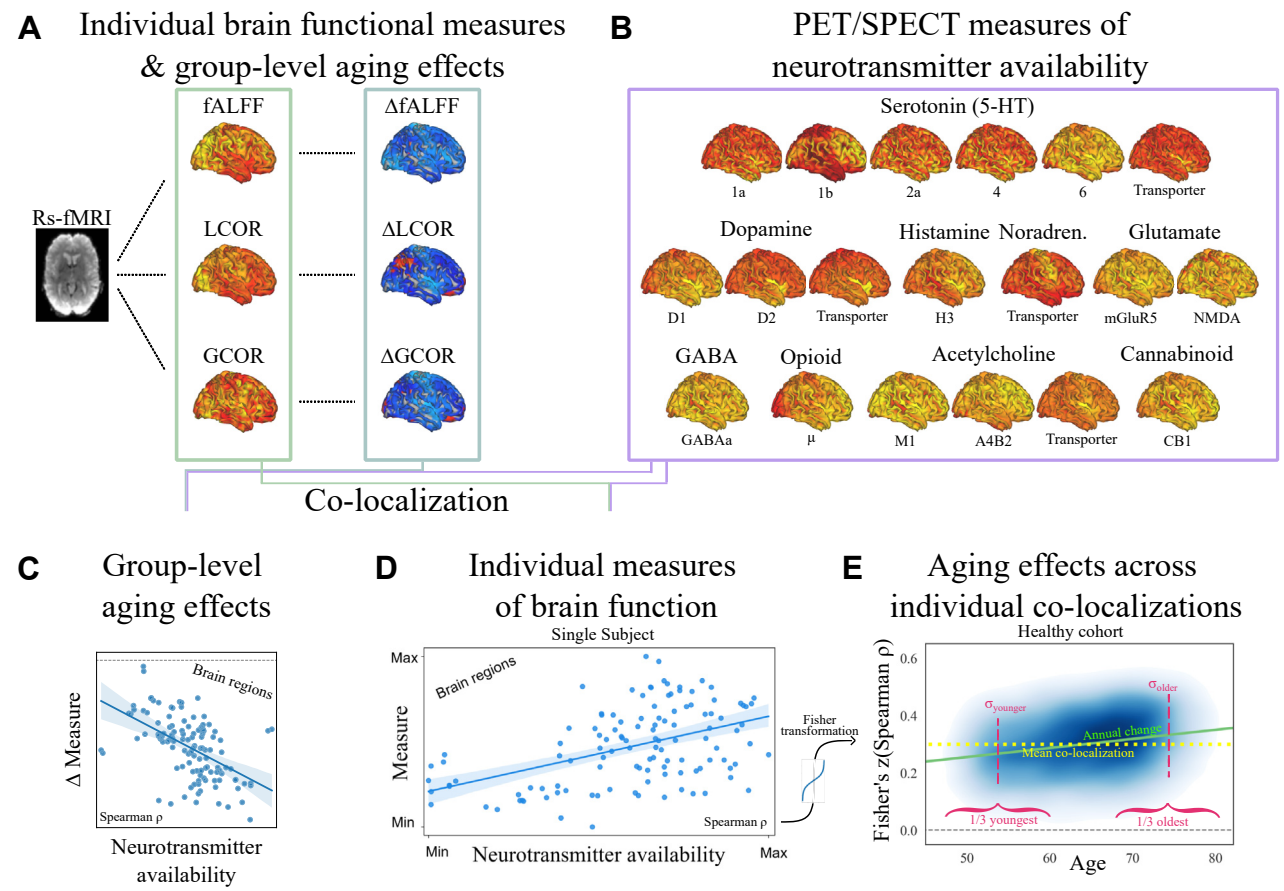

Figure 1. Methodological overview. We derived voxelwise maps of fALFF, LCOR, and GCOR from individual rs-fMRI data **(A)**. First, these data were used to explore group-level voxelwise aging changes in fALFF, LCOR, and GCOR in the healthy cohort ($n_{\text{healthy control}}$ = 25,917) (right column). **(B)** Second, we used PET maps of 19 neurotransmitter systems to calculate the spatial correlation (colocalization) with the **(C)** group-level aging effects and **(D)** individual fALFF, LCOR, and GCOR. **(E)** We Fisher's *z*-transformed the Spearman correlation coefficients ρ to ensure a normal distribution and examined the effects of age on the colocalization data of the healthy cohort. The blue cloud illustrates colocalization strengths (kernel density estimation of all transformed Spearman correlation coefficients) of the healthy cohort. For each pair of measure and neurotransmitter map, we analyzed mean colocalizations (yellow), linear aging effects (green), and differences in variances across participants in the youngest (44–60 years) and oldest (68–82 years) third of the sample (n_{Both} = 8639; red). Vertical dashed red lines were added for illustration purposes only and do not correspond to the actual variance of the respective subpopulation. **(F)** Next, we normatively modeled the colocalization strengths depending on age and sex (left) to calculate the deviation in participants with manifest PD (n_{PD} = 58; crosses). Here, we show the predicted means (solid lines) and 25% and 75% percentile (dashed lines) derived from the normative model for both men (blue) and women (orange). We analyzed whether the deviation (*z*) scores of participants with PD were significantly different from a null distribution (box plot). In this example, the distribution was significantly below a null distribution, indicating that patients with PD exhibited lower Spearman correlation coefficients than the norm. **(G)** Lastly, we quantified the mean regional contribution to the observed deviation score across participants with PD (left), as well as the functional differences in patients with PD compared to an age- and sex-matched subcohort of healthy control participants ($n_{\text{healthy control matched}}$ = 17,900) (right). The functional differences were quantified by calculating the regional effect sizes (Cohen's *d*). fALFF, fractional amplitude of low-frequency fluctuations; GABA, gamma-aminobutyric acid; GCOR, global correlation; LCOR, local correlation; PD, Parkinson's disease; PET, positron emission tomography; p_{FDR}, false discovery rate–corrected *p*; rs-fMRI, resting-state functional magnetic resonance imaging; SPECT, single photon emission computed tomography.

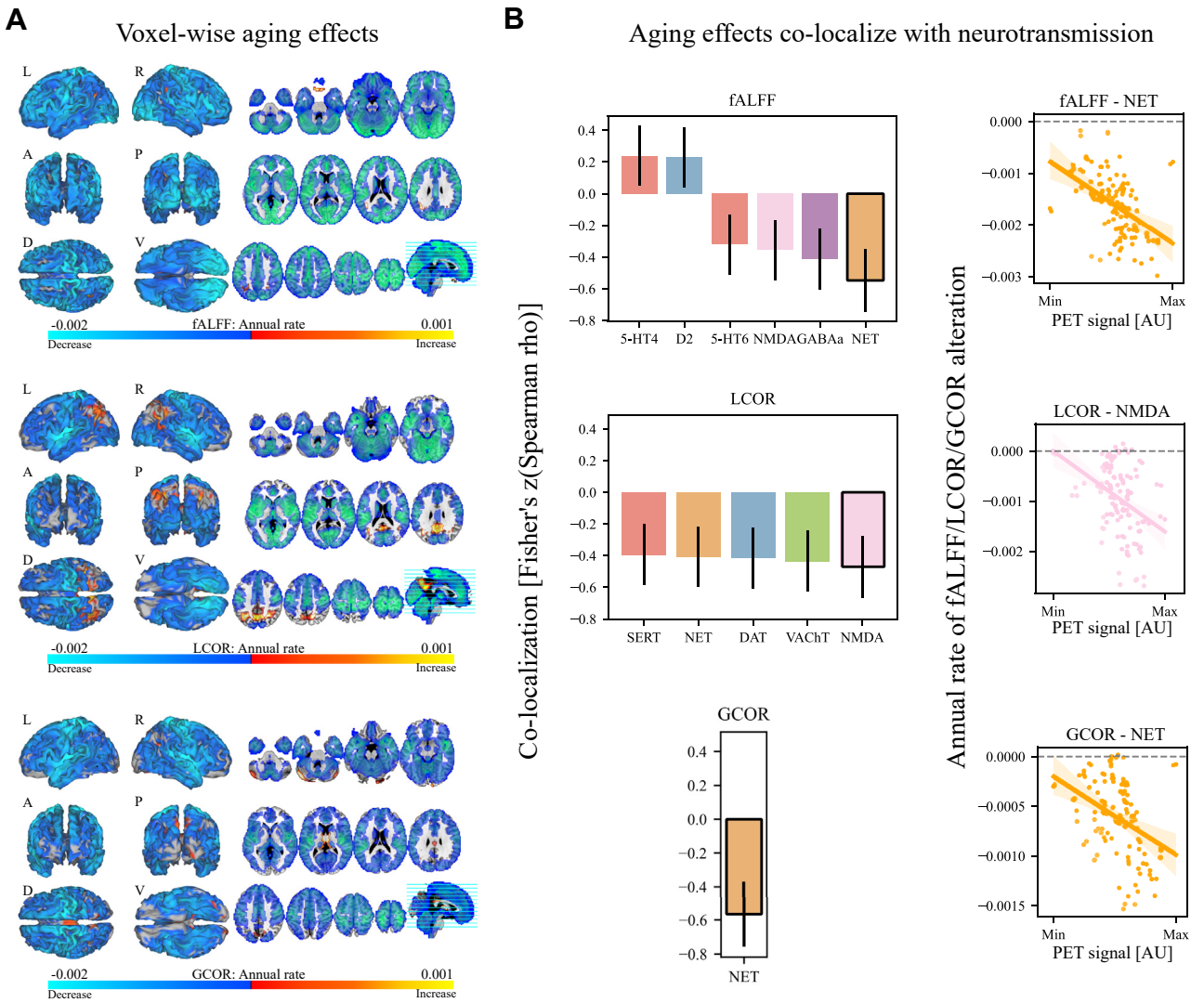

Figure 2. Group-level voxelwise aging effects for each functional measure and associations with neurotransmitter systems. **(A)** Colors in the voxelwise plots of thresholded group-level aging effects indicate annual decrease (blue) or increase (red) in fALFF (top), LCOR (middle), and GCOR (bottom). **(B)** Left column: significant ($p_{FDR} < .05$) linear correlations between annual rate in brain functional measure and neurotransmission. Vertical black lines indicate the uncertainty of Fisher's *z*-transformed Spearman correlation coefficient estimated according to Bonett and Wright (63). Right column: Exemplary scatterplots show how the annual change in fALFF, LCOR, or GCOR spatially correlate with the PET signal of specific neurotransmitter systems. Colors group receptors and transporters of the same neurotransmitter system, i.e., serotonin (red), dopamine (blue), acetylcholine (green), glutamate (pink), and GABA (purple), cannabinoid (mint), opioid (yellow), NET (orange), and histamine (turquoise). A, anterior; AU, arbitrary units; D, dorsal; DAT, dopamine transporter; fALFF, fractional amplitude of low-frequency fluctuations; GABA, gamma-aminobutyric acid; GCOR, global correlation; L, left; LCOR, local correlation; NET, norepinephrine transporter; P, posterior; PET, positron emission tomography; p_{FDR}, false discovery rate–corrected *p*; R, right; SERT, serotonin transporter; V, ventral; VAChT, vesicular acetylcholine transporter.

maps of age-related annual changes in all 3 measures and examined their spatial colocalization with the neurotransmitter systems. Annual changes in fALFF and LCOR were significantly correlated ($p_{FDR} < .05$) with serotonergic, dopaminergic, norepinephrinergic (also GCOR), and glutamate neurotransmission (Figure 2B; Figures S1 and S2; Tables S5 and S6). fALFF and LCOR changes correlated with GABAergic cholinergic neurotransmission, respectively. Except for the correlation between fALFF changes and NMDA, all findings remained significant after correcting for age-related atrophy. Scatterplots of the strongest correlations are shown in Figure 2B. Results for voxelwise sex differences are summarized in Figures S3–S5 and Tables S7–S10.

Individual Colocalization of Resting-State Measures and Neurotransmitter Systems Covaries With Age

The extent to which a specific neurotransmitter system contributed to the measured brain function was evaluated by its correlation strength. First, we computed individual

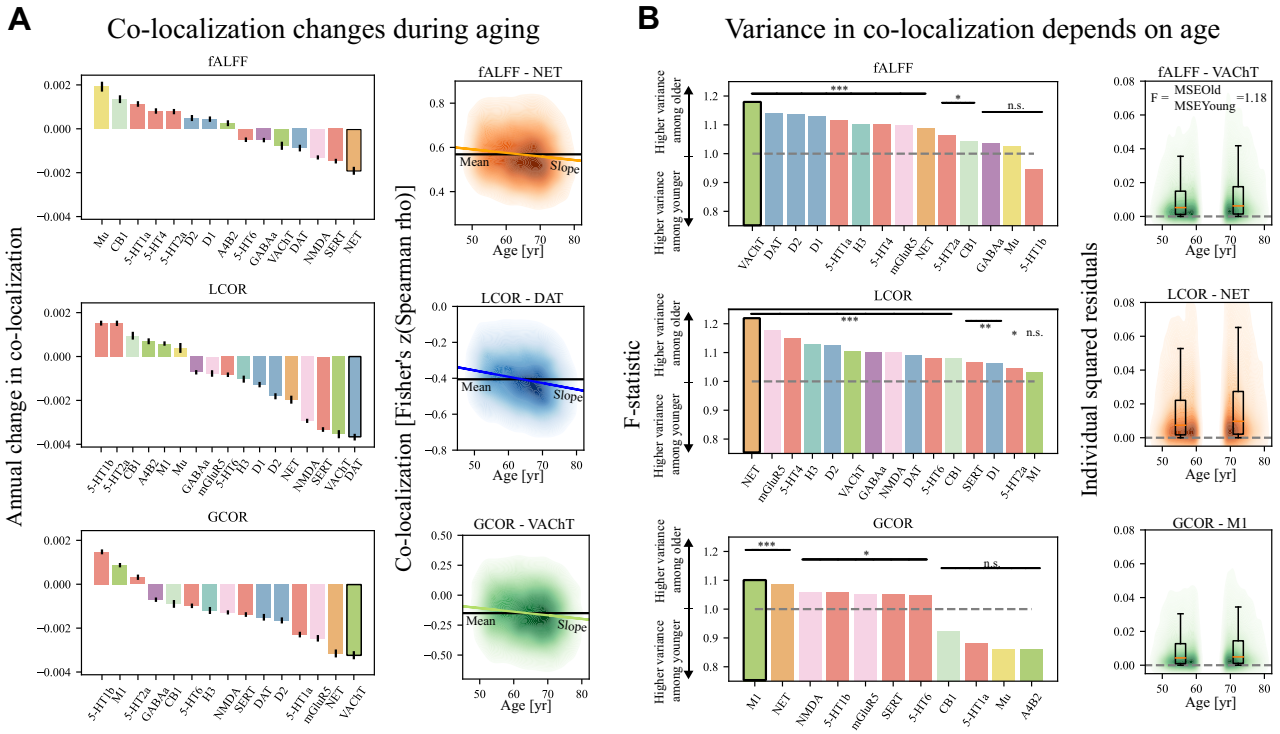

Figure 3. Single-participant colocalizations between brain functional measure and neurotransmitter systems depended on age. **(A)** Left column: overview of all significant linear aging effects ($p_{Bonferroni\text{-}Holm} < .05$) in the colocalization strengths (Fisher's *z*-transformed Spearman correlation coefficients) between each pair of brain functional measure (fALFF, LCOR, GCOR) and neurotransmitter system. Error bars correspond to the standard error of parameter (slope) estimation. Right column: Exemplary plots show how colocalization strengths between brain functional measures (fALFF, top; LCOR, middle; GCOR, bottom) and specific neurotransmitter systems depend on age. The black horizontal line indicates the population mean colocalization (see Figure S6 for an overview of all colocalization means). The colored clouds show the kernel density estimation of Fisher's *z*-transformed Spearman correlation coefficients of the healthy cohort. The slope of the colored line (linear fits) corresponds to the bar plots in the left column. **(B)** Left column: Each plot shows the effect size (*F* statistic) of MSE differences between younger and older adults. We show bar plots regarding neurotransmitter systems whose colocalization with the respective brain functional measure was previously shown to be significantly nonconstant (White test, $p_{FDR} < .05$). All pairs of brain function and PET map whose colocalization variance was significantly ($p_{FDR} < .05$) different in the older and the younger subpopulations are highlighted by asterisks (*$p_{FDR} < .05$, **$p_{FDR} < .01$, ***$p_{FDR} < .001$). *F* statistics (MSE of older adults divided by MSE of younger adults) above 1 correspond to a larger variance in the older subpopulation. Right column: Exemplary plots visualize the individual squared errors of the colocalizations between younger and older adults. Box plots show both distributions. Note that per definition, the squared errors are positive. Due to the kernel density estimation of all squared errors, the colored clouds exceed the null level. Colors group receptors and transporters of the same neurotransmitter system according to the same scheme as described in Figure 2. 5-HT, serotonin; DAT, dopamine transporter; fALFF, fractional amplitude of low-frequency fluctuation; GABA, gamma-aminobutyric acid; GCOR, global correlation; LCOR, local correlation; mGluR, metabotropic glutamate receptor; MSE, mean squared error; NET, norepinephrine transporter; n.s., not significant; PET, positron emission tomography; p_{FDR}, false discovery rate–corrected *p*; SERT, serotonin transporter; VAChT, vesicular acetylcholine transporter.

colocalization strengths between each participant's resting-state measure and each neurotransmitter map. Due to the large cohort size, even very small effects in all functional measures were significantly associated with the 19 PET maps (all $ps_{Bonferroni\text{-}Holm} < .001$, median absolute Spearman correlation coefficient ranged from 0.03 to 0.68), with different neurotransmitter systems explaining between 0.1% and 46% of the variance in the respective resting-state measures (Figure S6 and Tables S11–S13, left columns). The direction of the correlations was highly similar across the 3 measures. Positive correlations were found for the norepinephrinergic, muscarinic, glutamatergic, and GABAergic systems and serotonergic receptors 5-HT_{1B}, 5-HT_{2A}, and 5-HT_6. Negative correlations were found for the dopaminergic, histaminergic, and opioid neurotransmitter systems, serotonin receptors 5-HT_{1A} and 5-HT_4, and SERT and VAChT. All associations remained significant after controlling for age-related atrophy (Tables S14–S16). If age-related changes in brain functions are predominantly influenced by specific neurotransmitter systems, correlation coefficients should systematically (that is, in simplest approximation, linearly) increase or decrease during aging. Thus, we evaluated whether and to what extent aging effects and their colocalizations with neurotransmitter systems observed at the cohort level were also reflected in the individual colocalization strength. Most of the observed correlations were significantly associated, with age explaining up to 3%, 4%, and 1% of the colocalization strength between fALFF (with NMDA and SERT), LCOR (with SERT), and GCOR (with VAChT) and the respective neurotransmitter systems, respectively (Figure 3A; Tables S11–S13, middle columns). Correction for atrophy lowered the correlation strengths for most associations, but the findings remained largely significant (Tables S14–S16, middle columns).

Variance in Colocalization Changes During Aging

Because aging might not only have affected average colocalization strengths but might also have led to increased variance (i.e., due to undetected neurodegenerative processes in a subpopulation), we tested for such changes using a 2-step procedure. Using the White test, we identified significant nonconstant variance in colocalization strength. For fALFF and LCOR, nonconstant variance was observed for all neurotransmitter classes, except for LCOR and the opioid system. For GCOR, significant nonconstant variance in colocalization was found for serotoninergic, norepinephrinergic, cannabinoid, opioid, glutamatergic, and cholinergic neurotransmission (Table S17, left columns). These effects remained significant after controlling for atrophy except for GCOR and 5-HT_{1B}, 5-HT_6, and SERT (Table S18, left columns). Because the previous analysis only detected differences in variance across age but not their direction, we proceeded to perform the Goldfeld-Quandt test. Here, we compared the colocalization variance between the youngest (44–60 years) and oldest (68–82 years) third (n_{Both} = 8639) of the study population for the previously identified significant nonconstant variances (Figure 3B).

For fALFF and LCOR, higher variability in colocalization was found in the older subpopulation for serotonergic, dopaminergic, noradrenergic, histaminergic, cannabinoid, glutamatergic, and cholinergic neurotransmission. In addition, for LCOR, we found significantly higher variance in the older population in colocalization with the GABA system. For GCOR, higher variability in colocalization was found regarding the serotonergic, noradrenergic, glutamatergic, and cholinergic system. The number of neurotransmitter colocalization pairs, as identified using the White test, that showed a higher variance in the older subpopulation was 11 of 14 for fALFF, 14 of 15 for LCOR, and 7 of 11 for GCOR (Figure 3B; Table S17, right columns). The effects remained largely similar after controlling for atrophy (Table S18, right columns).

Deviations From Normal Colocalization in Manifest PD

Having established this reference for colocalization of normal age-related changes with different neurotransmitter systems, next we aimed to test whether and how functional changes caused by progressive neurodegeneration deviated from the nonpathological colocalization patterns. For this, we adopted a normative modeling approach using the healthy aging population as a reference (models are visualized in Figures S7 and S8). A UK Biobank subgroup of patients with PD served as an example for the clinical relevance of our findings. For fALFF, patients with PD had a lower colocalization strength with serotonergic, GABAergic, muscarinic, and glutamatergic neurotransmission (Figure 4D). For LCOR and GCOR, patients with PD showed lower colocalizations with serotonergic, dopaminergic, GABAergic, histaminergic, norepinephrinergic, glutamatergic, and cholinergic neurotransmitter systems (Figure 4E, F; Table S19). The deviation in colocalization strength regarding LCOR and $GABA_A$ (Figure 4A, B) was negatively correlated with disease duration, with higher deviations being indicative of longer disease duration (Pearson's $r = -0.38$, $p_{FDR} = .027$) (Figure 4C; Tables S21 and S22). No significant correlations were found between PD-related deviations in colocalization strengths and the cognitive score (cf. Tables S23–S29). After atrophy correction, all deviations remained significant except for the LCOR-5-HT_{1B} and LCOR-VAChT associations (Table S20).

Lastly, we aimed to understand which regions contributed most to the observed colocalization alterations in PD. For fALFF, the main contributing regions to colocalization changes in PD were the basal ganglia, insula, and occipital regions. For LCOR and GCOR, the main contributing regions were the basal ganglia, subcallosal areas, thalamus (LCOR only), and basal forebrain, as well as the pre- and postcentral insula and occipital regions (Figures S9–S11). The effects remained largely similar after controlling for atrophy (Figures S12–S14). Regional contribution to the deviations found regarding the glutamatergic system were significantly correlated with regional alteration in PD in both synchronicity measures ($p_{FDR} < .05$) (Figures S15 and S16; Tables S29 and S30; Figure 4G, H: effect sizes in regions with FDR-significant differences in LCOR and GCOR in PD vs. matched HC; Tables S31 and S32: regional comparison of fALFF, LCOR, and GCOR in patients with PD vs. matched HCs; Figures S17–S19: regional effect sizes in fALFF, LCOR, and GCOR in patients with PD vs. matched HCs).

DISCUSSION

In the current study, we tested how age-related changes in commonly applied resting activity and connectivity measures colocalize with underlying neurotransmission. Consistent with previous studies of aging effects on brain function, we found widespread age-related decreases but also several increases in the 3 evaluated measures (2,3,66). These age-related changes showed a robust colocalization pattern with various major neurotransmitter systems, including monoamines, glutamate, acetylcholine, and GABA, at the group- and single-participant level. Variance in the colocalization patterns of these systems increased with age. Patients with PD showed significant deviations from typical age-related colocalization patterns in neurotransmitter systems related to the disease. The deviation in colocalization strength regarding the GABAergic system was correlated with disease duration.

Consistent with most studies that have reported aging effects in the brain, we found widespread age-related decreases in all 3 evaluated functional measures (1–5). The extent of the decreases is substantially higher in our study, covering basically all of the brain, with few exceptions as discussed below. Considering the large cohort size, the increased statistical power compared with previous studies with at most a few hundred participants is the most likely explanation for the observed discrepancy. In parallel, we observed spatially distinct age-related increases across the 3 evaluated measures covering parietal, precuneal, thalamic, gyrus rectus, and cerebellar regions. Recent theories of neurocognitive aging including dedifferentiation (67) and scaffolding (68) may provide potential explanations for these patterns of brain functional alteration. Neuronal compensation and inefficiency may be associated with increased or decreased cognitive functioning, respectively (69,70). With respect to directionality, our findings are consistent with several previous studies suggesting presumably compensation-related increases in

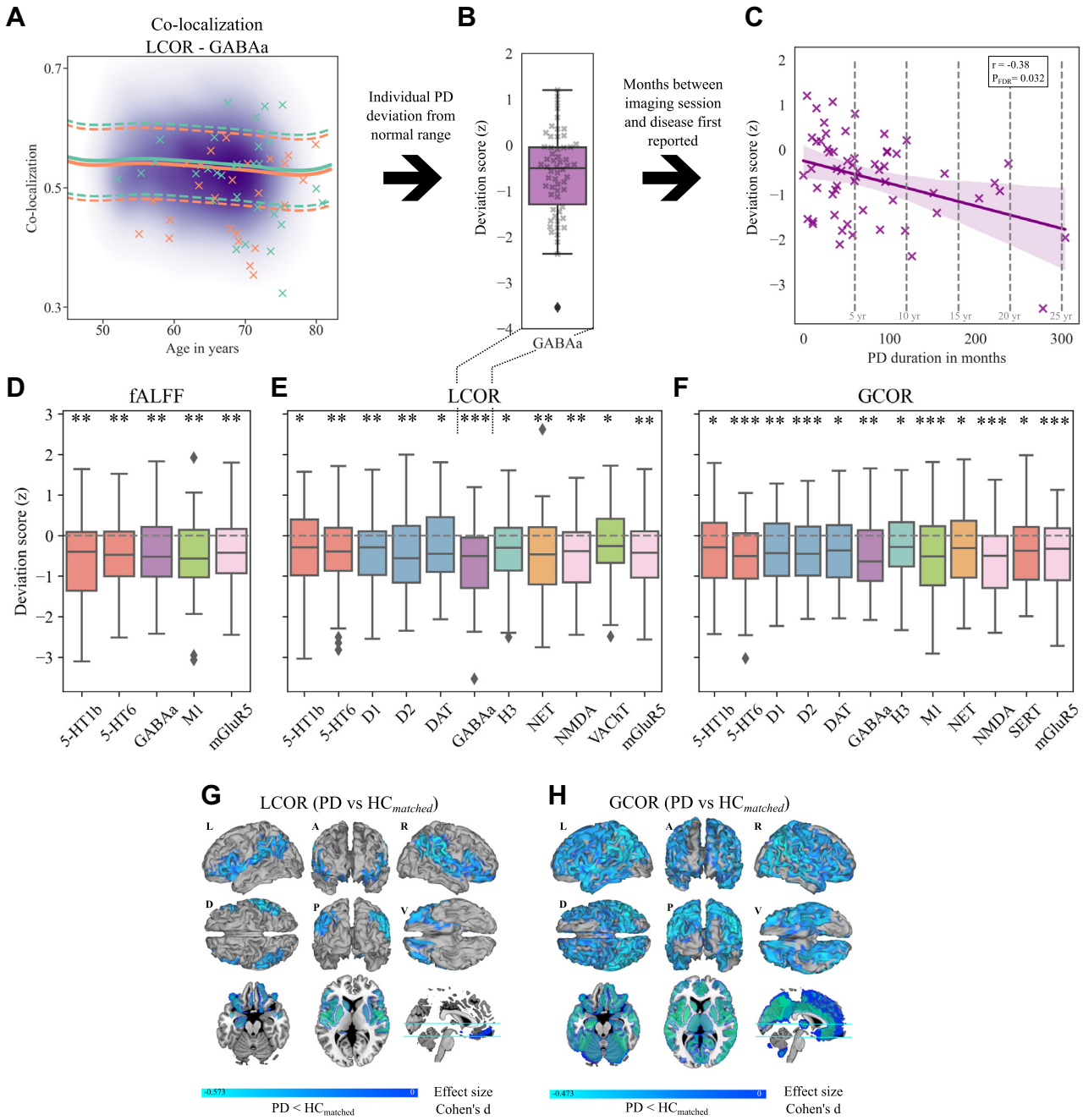

Figure 4. Participants with PD deviated from normative models of colocalization between brain function and neurotransmitter systems. **(A)** The purple cloud shows the kernel density plot of Fisher's *z*-transformed Spearman correlation coefficients of the healthy cohort regarding the spatial correlation of LCOR and $GABA_A$. Solid and dashed lines show the predicted mean and predicted 25% or 75% percentile of men (turquoise) and women (orange) derived from the normative models. Crosses indicate the colocalization levels of patients with PD. **(B)** Box plot showing the significant deviation from the norm (null) in patients with PD. **(C)** Deviation scores in the PD group were significantly correlated with disease duration. **(D–F)** Box plots showing the deviation scores that were significantly different from the norm (null) regarding **(D)** fALFF, **(E)** LCOR, and **(F)** GCOR. *, **, and *** indicate Bonferroni-Holm–corrected significant deviations of the distributions from a null distribution with exact $p < .05$, $p < .01$, and $p < .001$. Colors in box plots group receptors and transporters of the same neurotransmitter system according to the same scheme as described in Figure 2. **(G, H)** Significant ($p_{FDR} < .05$) regional differences (effect sizes, Cohen's *d*) between the PD group and the matched subgroup of HCs in **(G)** LCOR and **(H)** GCOR. Lower values in the PD group are indicated by blue areas. Effect sizes of all regions are provided in Figures S17–S19. 5-HT, serotonin; DAT, dopamine transporter; fALFF, fractional amplitude of low-frequency fluctuations; $GABA_A$, gamma-aminobutyric acid A; GCOR, global correlation; HC, healthy control participant; L, left; LCOR, local correlation; mGluR, metabotropic glutamate receptor; NET, norepinephrine transporter; P, posterior; PD, Parkinson's disease; p_{FDR}, false discovery rate–corrected *p*; R, right; SERT, serotonin transporter; V, ventral; VAChT, vesicular acetylcholine transporter.

different connectivity metrics in the aging population (66,71). However, such locally restricted increases and the observed global decreases may also be attributed to a loss of functional differentiation leading to unorganized additional activation or suppression across different regions or to reduced neural efficiency leading to an inability to suppress specific activation patterns (69).

Supporting the previously reported complex reorganization of the excitation/inhibition balance during aging (72), we found that the group-level aging effects on brain function were associated with glutamatergic and GABAergic neurotransmission. The additional colocalization of the aging effects with monoaminergic and cholinergic systems may support the idea that the underlying changes are related to learning, memory, and other higher cognitive functions affected by aging (7,15,71,73). In contrast, age-related global connectivity primarily increased in thalamic and cerebellar regions, and the topography of these changes only aligns with norepinephrinergic neurotransmission. Both regions and in particular the thalamus show a high expression of norepinephrine receptors (74,75). While the modulatory role of norepinephrine in the cerebellum has been repeatedly associated with motor learning (76,77), its contribution to aging is controversial, with its activity being associated with prevention but also acceleration of the production and accumulation of amyloid-β and tau across the brain (78). On a functional level, these findings may be related to the functional decline of the norepinephrinergic system, which is considered to be a key factor in maintaining arousal and cognitive adaptation and control (79,80).

When testing for colocalization of functional measures with neurotransmission at the single-participant level, we found that age-related alterations in all 3 measures colocalized primarily with monoaminergic neurotransmission. Increases in variance observed for a variety of evaluated neurotransmitter systems complemented these findings. Considering the reportedly high prevalence of neuropathology in a cognitively normal older population (81,82), the individual colocalization changes—together with increased variance—may reflect such still undetected neurodegenerative processes. To test the sensitivity of the colocalization patterns to such neurodegenerative processes, we further adopted a normative modeling approach. A major advantage of normative models is their ability to represent population heterogeneity in the phenotype under investigation by means of normalized deviation scores (64). We applied this approach in patients with a diagnosis of PD, which was previously linked to monoaminergic neurotransmission as well as more recently to an imbalance between GABA and glutamate (83–85). In patients with PD, colocalization patterns significantly deviated from age- and sex-adjusted normative models across various neurotransmitter systems and all 3 functional metrics. Deviations in local activity colocalization were found primarily with respect to serotonergic, GABA, and glutamatergic neurotransmission, while deviations in colocalization of both connectivity measures were also present with respect to dopamine neurotransmission. We found that only the deviation in colocalization strength of local connectivity with $GABA_A$ receptors predicted disease duration, thereby supporting the suggested relevance of GABA pathology for clinical progression (83). The observed age-related increases in variance regarding GABAergic colocalization with brain function supports the notion of its contribution to potential pathophysiological changes in parts of the aging population. This interpretation is also supported by its association with disease duration in patients with PD in our study. Consistent with that, GABAergic system changes have recently been reported in PD and were associated with visual hallucinations and axial symptoms (such as postural instability, rigidity, and bradykinesia) (86–88). The observed distinct colocalization patterns of various neurotransmitter systems with functional changes in aging and PD point to distinct pathophysiological processes affecting the respective processes. Such insights, if confirmed by other modalities, may help with identification of novel drug targets as well as development of successful monitoring strategies for the respective pathophysiological changes.

The studied cohort was recruited as a representative sample of healthy UK residents. Because the metrics target local brain function, participants with diseases primarily affecting brain structure or function were excluded. Given the prevalence of mild depressive symptoms in the UK population of 11% (89) and the fact that 12.32% of our analyzed participants from the UK Biobank have a reference to ICD-10: F32, their exclusion would have biased the cohort. PD appearance and progression is highly heterogeneous. Because no scores for PD severity [i.e., Unified Parkinson's Disease Rating Scale (90) or Hoehn & Yahr stages (91)] and only a limited number of cognitive scores were available, we could only roughly approximate PD severity based on disease duration. Because PD medication is known to affect measures of brain function, it might have contributed to some of the effects observed in the PD cohort in the current study. However, the effects of PD medication on spatial colocalization have previously been shown to be rather negligible compared with the effects of PD (25). Additional healthy control biases in the UK Biobank (92) include a high average socioeconomic status and low alcohol and tobacco consumption. Although socioeconomic status may be associated with cognitive reserve through strengthened cognitive abilities during childhood (93,94), we estimate that deviations from the overall population results are small with respect to these primary biases. Further sampling of a more diverse population is needed to address the potential impact of such biases. Clinical scores of disease severity should be used to strengthen evidence for the observed association with GABAergic neurotransmission. Using PET maps from differently aged healthy populations might have introduced a further bias into our findings because proteomics such as receptor and transporter distributions may change during aging (79,95).

Conclusions

Here, we provided a detailed overview on aging effects on macroscopic brain functioning as observed using common rs-fMRI-derived measures of local activity and local and global connectivity. We linked these age-related changes to the distribution of various neurotransmitter systems, demonstrating a decline in colocalization strength together with increased variance during aging. By adopting a normative modeling approach to the example of PD, we further demonstrated the feasibility of using colocalization strength as a sensitive

measure of neurodegeneration, thus providing potentially valuable insight into the underlying neuropathological processes.

ACKNOWLEDGMENTS AND DISCLOSURES

This work was supported by the European Union's Horizon 2020 research and innovation program (Grant No. 826421 [to JD]); TheVirtualBrain-Cloud; the European Union's Horizon 2020 research and innovation program (Grant No. 945539 [to SC and SBE]) (Human Brain Project SGA3); and the Federal Ministry of Education and Research and the Max Planck Society, Germany (to LDL).

We are grateful for the immense work of the whole UK Biobank team, as well as all the volunteers who contributed to this dataset of inestimable value. This research has been conducted using the UK Biobank Resource under Application Number 41655.

The authors report no biomedical financial interests or potential conflicts of interest.

ARTICLE INFORMATION

From the Institute of Systems Neuroscience, Medical Faculty and University Hospital Düsseldorf, Heinrich-Heine-Universität Düsseldorf, Düsseldorf, Germany (JK, LDL, FH, SBE, JD); Institute of Neuroscience and Medicine (INM-7), Research Centre Jülich, Jülich, Germany (JK, LDL, FH, SBE, JD); Institute for Anatomy I, Medical Faculty and University Hospital Düsseldorf, Heinrich-Heine-Universität Düsseldorf, Düsseldorf, Germany (SC); Institute of Neuroscience and Medicine (INM-1), Research Centre Jülich, Jülich, Germany (SC); and Max Planck School of Cognition, Leipzig, Germany (LDL).

Address correspondence to Juergen Dukart, Ph.D., at j.dukart@fz-juelich.de.

Received Jan 14, 2024; revised Mar 15, 2024; accepted Apr 16, 2024.

Supplementary material cited in this article is available online at https://doi.org/10.1016/j.bpsc.2024.04.010.

REFERENCES

1. Biswal BB, Mennes M, Zuo X-N, Gohel S, Kelly C, Smith SM, *et al.* (2010): Toward discovery science of human brain function. Proc Natl Acad Sci USA 107:4734–4739.
2. Hu S, Chao HH-A, Zhang S, Ide JS, Li C-SR (2014): Changes in cerebral morphometry and amplitude of low-frequency fluctuations of BOLD signals during healthy aging: Correlation with inhibitory control. Brain Struct Funct 219:983–994.
3. Vieira BH, Rondinoni C, Garrido Salmon CE (2020): Evidence of regional associations between age-related inter-individual differences in resting-state functional connectivity and cortical thinning revealed through a multi-level analysis. Neuroimage 211:116662.
4. Montalà-Flaquer M, Cañete-Massé C, Vaqué-Alcázar L, Bartrés-Faz D, Peró-Cebollero M, Guàrdia-Olmos J (2022): Spontaneous brain activity in healthy aging: An overview through fluctuations and regional homogeneity. Front Aging Neurosci 14:1002811.
5. Wu T, Zang Y, Wang L, Long X, Li K, Chan P (2007): Normal aging decreases regional homogeneity of the motor areas in the resting state. Neurosci Lett 423:189–193.
6. Harrison TM, Maass A, Adams JN, Du R, Baker SL, Jagust WJ (2019): Tau deposition is associated with functional isolation of the hippocampus in aging. Nat Commun 10:4900.
7. Karrer TM, McLaughlin CL, Guaglianone CP, Samanez-Larkin GR (2019): Reduced serotonin receptors and transporters in normal aging adults: A meta-analysis of PET and SPECT imaging studies. Neurobiol Aging 80:1–10.
8. Sheline YI, Mintun MA, Moerlein SM, Snyder AZ (2002): Greater loss of 5-HT_{2A} receptors in midlife than in late life. Am J Psychiatry 159:430–435.
9. Nord M, Cselenyi Z, Forsberg A, Rosenqvist G, Tiger M, Lundberg J, *et al.* (2014): Distinct regional age effects on [^{11}C]AZ10419369 binding to 5-HT1B receptors in the human brain. Neuroimage 103:303–308.
10. Madsen K, Haahr MT, Marner L, Keller SH, Baaré WF, Svarer C, *et al.* (2011): Age and sex effects on 5-HT_4 receptors in the human brain: A [^{11}C]SB207145 PET study. J Cereb Blood Flow Metab 31:1475–1481.
11. Radhakrishnan R, Nabulsi N, Gaiser E, Gallezot J-D, Henry S, Planeta B, *et al.* (2018): Age-related change in 5-HT_6 receptor availability in healthy male volunteers measured with ^{11}C-GSK215083 PET. J Nucl Med 59:1445–1450.
12. Antonini A, Leenders KL, Reist H, Thomann R, Beer HF, Locher J (1993): Effect of age on D2 dopamine receptors in normal human brain measured by positron emission tomography and 11C-Raclopride. Arch Neurol 50:474–480.
13. Seaman KL, Smith CT, Juarez EJ, Dang LC, Castrellon JJ, Burgess LL, *et al.* (2019): Differential regional decline in dopamine receptor availability across adulthood: Linear and nonlinear effects of age. Hum Brain Mapp 40:3125–3138.
14. Wang Y, Chan GLY, Holden JE, Dobko T, Mak E, Schulzer M, *et al.* (1998): Age-dependent decline of dopamine D1 receptors in human brain: A PET study. Synapse 30:56–61.
15. Karrer TM, Josef AK, Mata R, Morris ED, Samanez-Larkin GR (2017): Reduced dopamine receptors and transporters but not synthesis capacity in normal aging adults: A meta-analysis. Neurobiol Aging 57:36–46.
16. Magnusson KR (2010): Selective vulnerabilities of N-methyl-D-aspartate (NMDA) receptors during brain aging. FrontiAgNeurosci 2:11.
17. Perry EK, Piggott MA, Court JA, Johnson M, Perry RH (1993): Transmitters in the developing and senescent human brain. Ann N Y Acad Sci 695:69–72.
18. Piggott MA, Perry EK, Perry RH, Court JA (1992): [^{3}H]MK-801 binding to the NMDA receptor complex, and its modulation in human frontal cortex during development and aging. Brain Res 588:277–286.
19. Zubieta JK, Koeppe RA, Frey KA, Kilbourn MR, Mangner TJ, Foster NL, Kuhl DE (2001): Assessment of muscarinic receptor concentrations in aging and Alzheimer disease with [11C]NMPB and PET. Synapse 39:275–287.
20. Ding Y-S, Singhal T, Planeta-Wilson B, Gallezot J-D, Nabulsi N, Labaree D, *et al.* (2010): PET imaging of the effects of age and cocaine on the norepinephrine transporter in the human brain using (S,S)-[^{11}C]O-methylreboxetine and HRRT. Synapse 64:30–38.
21. Cuypers K, Hehl M, Van Aalst J, Chalavi S, Mikkelsen M, Van Laere K, *et al.* (2021): Age-related GABAergic differences in the primary sensorimotor cortex: A multimodal approach combining PET, MRS and TMS. Neuroimage 226:117536.
22. Zubieta JK, Dannals RF, Frost JJ (1999): Gender and age influences on human brain mu-opioid receptor binding measured by PET. Am J Psychiatry 156:842–848.
23. Hansen JY, Shafiei G, Markello RD, Smart K, Cox SML, Nørgaard M, *et al.* (2022): Mapping neurotransmitter systems to the structural and functional organization of the human neocortex. Nat Neurosci 25:1569–1581.
24. Dukart J, Holiga Š, Chatham C, Hawkins P, Forsyth A, McMillan R, *et al.* (2018): Cerebral blood flow predicts differential neurotransmitter activity. Sci Rep 8:4074.
25. Dukart J, Holiga S, Rullmann M, Lanzenberger R, Hawkins PCT, Mehta MA, *et al.* (2021): JuSpace: A tool for spatial correlation analyses of magnetic resonance imaging data with nuclear imaging derived neurotransmitter maps. Hum Brain Mapp 42:555–566.
26. Marquand AF, Haak KV, Beckmann CF (2017): Functional corticostriatal connection topographies predict goal directed behaviour in humans. Nat Hum Behav 1:0146.
27. Wolfers T, Beckmann CF, Hoogman M, Buitelaar JK, Franke B, Marquand AF (2020): Individual differences *v.* the average patient: Mapping the heterogeneity in ADHD using normative models. Psychol Med 50:314–323.
28. Fraza CJ, Dinga R, Beckmann CF, Marquand AF (2021): Warped Bayesian linear regression for normative modelling of big data. Neuroimage 245:118715.
29. Ziegler G, Ridgway GR, Dahnke R, Gaser C, Alzheimer's Disease Neuroimaging Initiative (2014): Individualized Gaussian process-based

prediction and detection of local and global gray matter abnormalities in elderly subjects. Neuroimage 97:333–348.
30. Kaasinen V, Vahlberg T, Stoessl AJ, Strafella AP, Antonini A (2021): Dopamine receptors in Parkinson's disease: A meta-analysis of imaging studies. Mov Disord 36:1781–1791.
31. Kaasinen V, Någren K, Hietala J, Oikonen V, Vilkman H, Farde L, *et al.* (2000): Extrastriatal dopamine D2 and D3 receptors in early and advanced Parkinson's disease. Neurology 54:1482–1487.
32. Seeman P, Niznik HB (1990): Dopamine receptors and transporters in Parkinson's disease and schizophrenia. FASEB J 4:2737–2744.
33. Politis M, Piccini P, Pavese N, Koh S-B, Brooks DJ (2008): Evidence of dopamine dysfunction in the hypothalamus of patients with Parkinson's disease: An in vivo ^{11}C-raclopride PET study. Exp Neurol 214:112–116.
34. Takashima H, Terada T, Bunai T, Matsudaira T, Obi T, Ouchi Y (2022): In vivo illustration of altered dopaminergic and GABAergic systems in early Parkinson's disease. Front Neurol 13:880407.
35. Yao N-T, Zheng Q, Xu Z-Q, Yin J-H, Lu L-G, Zuo Q, *et al.* (2020): Positron emission computed tomography/single photon emission computed tomography in Parkinson disease. Chin Med J (Engl) 133:1448–1455.
36. Huot P, Fox SH, Brotchie JM (2011): The serotonergic system in Parkinson's disease. Prog Neurobiol 95:163–212.
37. Melse M, Tan SKH, Temel Y, van Kroonenburgh MJPG, Leentjens AFG (2014): Changes in 5-HT_{2A} receptor expression in untreated, de novo patients with Parkinson's disease. J Parkinsons Dis 4:283–287.
38. Varrone A, Svenningsson P, Forsberg A, Varnäs K, Tiger M, Nakao R, *et al.* (2014): Positron emission tomography imaging of 5-hydroxytryptamine$_{1B}$ receptors in Parkinson's disease. Neurobiol Aging 35:867–875.
39. Kang Y, Henchcliffe C, Verma A, Vallabhajosula S, He B, Kothari PJ, *et al.* (2019): 18F-FPEB PET/CT shows mGluR5 upregulation in Parkinson's disease. J Neuroimaging 29:97–103.
40. Zhang Z, Zhang S, Fu P, Zhang Z, Lin K, Ko JK-S, Yung KK-L (2019): Roles of glutamate receptors in Parkinson's disease. Int J Mol Sci 20:4391.
41. Sharma A, Muresanu DF, Patnaik R, Menon PK, Tian ZR, Sahib S, *et al.* (2021): Histamine H3 and H4 receptors modulate Parkinson's disease induced brain pathology. Neuroprotective effects of nanowired BF-2649 and clobenpropit with anti-histamine-antibody therapy. Prog Brain Res 266:1–73.
42. Meyer PM, Tiepolt S, Barthel H, Hesse S, Sabri O (2014): Radioligand imaging of α4β2* nicotinic acetylcholine receptors in Alzheimer's disease and Parkinson's disease. Q J Nucl Med Mol Imaging 58:376–386.
43. Asahina M, Suhara T, Shinotoh H, Inoue O, Suzuki K, Hattori T (1998): Brain muscarinic receptors in progressive supranuclear palsy and Parkinson's disease: A positron emission tomographic study. J Neurol Neurosurg Psychiatry 65:155–163.
44. van der Zee S, Kanel P, Gerritsen MJJ, Boertien JM, Slomp AC, Müller MLTM, *et al.* (2022): Altered cholinergic innervation in de novo Parkinson's disease with and without cognitive impairment. Mov Disord 37:713–723.
45. Nahimi A, Kinnerup MB, Sommerauer M, Gjedde A, Borghammer P (2018): Molecular imaging of the noradrenergic system in idiopathic Parkinson's disease. Int Rev Neurobiol 141:251–274.
46. Brumberg J, Tran-Gia J, Lapa C, Isaias IU, Samnick S (2019): PET imaging of noradrenaline transporters in Parkinson's disease: Focus on scan time. Ann Nucl Med 33:69–77.
47. Smith SM, Alfaro-Almagro F, Miller KL (2020): UK Biobank Brain Imaging Documentation (version 1.8). Available at: https://biobank.ctsu.ox.ac.uk/crystal/crystal/docs/brain_mri.pdf. Accessed February 13, 2023.
48. Zou Q-H, Zhu C-Z, Yang Y, Zuo X-N, Long X-Y, Cao Q-J, *et al.* (2008): An improved approach to detection of amplitude of low-frequency fluctuation (ALFF) for resting-state fMRI: Fractional ALFF. J Neurosci Methods 172:137–141.
49. Deshpande G, LaConte S, Peltier S, Hu X (2009): Integrated local correlation: A new measure of local coherence in fMRI data. Hum Brain Mapp 30:13–23.
50. Saad ZS, Reynolds RC, Jo HJ, Gotts SJ, Chen G, Martin A, Cox RW (2013): Correcting brain-wide correlation differences in resting-state FMRI. Brain Connect 3:339–352.
51. Kasper J, Eickhoff SB, Caspers S, Peter J, Dogan I, Wolf RC, *et al.* (2023): Local synchronicity in dopamine-rich caudate nucleus influences Huntington's disease motor phenotype. Brain 146:3319–3330.
52. Beliveau V, Ganz M, Feng L, Ozenne B, Højgaard L, Fisher PM, *et al.* (2017): A high-resolution *in vivo* atlas of the human Brain's serotonin system. J Neurosci 37:120–128.
53. Gallezot J-D, Nabulsi N, Neumeister A, Planeta-Wilson B, Williams WA, Singhal T, *et al.* (2010): Kinetic modeling of the serotonin 5-HT_{1B} receptor radioligand [^{11}C]P943 in humans. J Cereb Blood Flow Metab 30:196–210.
54. Kaller S, Rullmann M, Patt M, Becker G-A, Luthardt J, Girbardt J, *et al.* (2017): Test–retest measurements of dopamine D_1-type receptors using simultaneous PET/MRI imaging. Eur J Nucl Med Mol Imaging 44:1025–1032.
55. Sandiego CM, Gallezot J-D, Lim K, Ropchan J, Lin SF, Gao H, *et al.* (2015): Reference region modeling approaches for amphetamine challenge studies with [^{11}C]FLB 457 and PET. J Cereb Blood Flow Metab 35:623–629.
56. Gallezot J-D, Planeta B, Nabulsi N, Palumbo D, Li X, Liu J, *et al.* (2017): Determination of receptor occupancy in the presence of mass dose: [^{11}C]GSK189254 PET imaging of histamine H3 receptor occupancy by PF-03654746. J Cereb Blood Flow Metab 37:1095–1107.
57. Aghourian M, Legault-Denis C, Soucy JP, Rosa-Neto P, Gauthier S, Kostikov A, *et al.* (2017): Quantification of brain cholinergic denervation in Alzheimer's disease using PET imaging with [^{18}F]-FEOBV. Mol Psychiatry 22:1531–1538.
58. Naganawa M, Nabulsi N, Henry S, Matuskey D, Lin S-F, Slieker L, *et al.* (2021): First-in-human assessment of ^{11}C-LSN3172176, an M1 muscarinic acetylcholine receptor PET radiotracer. J Nucl Med 62:553–560.
59. Hillmer AT, Esterlis I, Gallezot JD, Bois F, Zheng MQ, Nabulsi N, *et al.* (2016): Imaging of cerebral $\alpha_4\beta_2$* nicotinic acetylcholine receptors with (−)-[^{18}F]Flubatine PET: Implementation of bolus plus constant infusion and sensitivity to acetylcholine in human brain. Neuroimage 141:71–80.
60. Smart K, Cox SML, Scala SG, Tippler M, Jaworska N, Boivin M, *et al.* (2019): Sex differences in [^{11}C]ABP688 binding: A positron emission tomography study of mGlu5 receptors. Eur J Nucl Med Mol Imaging 46:1179–1183.
61. Galovic M, Al-Diwani A, Vivekananda U, Torrealdea F, Erlandsson K, Fryer TD, *et al.* (2021): In vivo NMDA receptor function in people with NMDA receptor antibody encephalitis. medRxiv. https://doi.org/10.1101/2021.12.04.21267226.
62. Normandin MD, Zheng M-Q, Lin K-S, Mason NS, Lin S-F, Ropchan J, *et al.* (2015): Imaging the cannabinoid CB1 receptor in humans with [^{11}C]OMAR: Assessment of kinetic analysis methods, test-retest reproducibility, and gender differences. J Cereb Blood Flow Metab 35:1313–1322.
63. Bonett DG, Wright TA (2000): Sample size requirements for estimating Pearson, Kendall and spearman correlations. Psychometrika 65:23–28.
64. Rutherford S, Kia SM, Wolfers T, Fraza C, Zabihi M, Dinga R, *et al.* (2022): The normative modeling framework for computational psychiatry. Nat Protoc 17:1711–1734.
65. Lotter LD, Saberi A, Hansen JY, Misic B, Paquola C, Barker GJ, *et al.* (2023): Human cortex development is shaped by molecular and cellular brain systems. bioRxiv. https://doi.org/10.1101/2023.05.05.539537.
66. Vij SG, Nomi JS, Dajani DR, Uddin LQ (2018): Evolution of spatial and temporal features of functional brain networks across the lifespan. Neuroimage 173:498–508.
67. Koen JD, Rugg MD (2019): Neural dedifferentiation in the aging brain. Trends Cogn Sci 23:547–559.
68. Reuter-Lorenz PA, Park DC (2014): How does it STAC up? Revisiting the scaffolding theory of aging and cognition. Neuropsychol Rev 24:355–370.

69. McDonough IM, Nolin SA, Visscher KM (2022): 25 years of neurocognitive aging theories: What have we learned? Front Aging Neurosci 14:1002096.
70. Bunzeck N, Steiger TK, Krämer UM, Luedtke K, Marshall L, Obleser J, Tune S (2024): Trajectories and contributing factors of neural compensation in healthy and pathological aging. Neurosci Biobehav Rev 156:105489.
71. Behfar Q, Behfar SK, Von Reutern B, Richter N, Dronse J, Fassbender R, *et al.* (2020): Graph theory analysis reveals resting-state compensatory mechanisms in healthy aging and prodromal Alzheimer's disease. Front Aging Neurosci 12:576627.
72. Petitet P, Spitz G, Emir UE, Johansen-Berg H, O'Shea J (2021): Age-related decline in cortical inhibitory tone strengthens motor memory. Neuroimage 245:118681.
73. Bernier M, Croteau E, Castellano C-A, Cunnane SC, Whittingstall K (2017): Spatial distribution of resting-state BOLD regional homogeneity as a predictor of brain glucose uptake: A study in healthy aging. Neuroimage 150:14–22.
74. Oke AF, Carver LA, Gouvion CM, Adams RN (1997): Three-dimensional mapping of norepinephrine and serotonin in human thalamus. Brain Res 763:69–78.
75. Zitnik G, Chandler DJ, Waterhouse BD (2016): Norepinephrine and synaptic transmission in the cerebellum. In: Gruol DL, Koibuchi N, Manto M, Molinari M, Schmahmann JD, Shen Y, editors. Essentials of Cerebellum and Cerebellar Disorders. Cham, Germany: Springer International Publishing, 237–241.
76. Cartford MC, Gould T, Bickford PC (2004): A central role for norepinephrine in the modulation of cerebellar learning tasks. Behav Cogn Neurosci Rev 3:131–138.
77. Bickford P (1995): Aging and motor learning: A possible role for norepinephrine in cerebellar plasticity. Rev Neurosci 6:35–46.
78. Mather M (2021): Noradrenaline in the aging brain: Promoting cognitive reserve or accelerating Alzheimer's disease? Semin Cell Dev Biol 116:108–124.
79. Lee J, Kim H-J (2022): Normal aging induces changes in the brain and neurodegeneration progress: Review of the structural, biochemical, metabolic, cellular, and molecular changes. Front Aging Neurosci 14: 931536.
80. Guedj C, Monfardini E, Reynaud AJ, Farnè A, Meunier M, Hadj-Bouziane F (2017): Boosting norepinephrine transmission triggers flexible reconfiguration of brain networks at rest. Cereb Cortex 27:4691–4700.
81. Chételat G, La Joie R, Villain N, Perrotin A, De La Sayette V, Eustache F, Vandenberghe R (2013): Amyloid imaging in cognitively normal individuals, at-risk populations and preclinical Alzheimer's disease. Neuroimage Clin 2:356–365.
82. Markesbery WR, Jicha GA, Liu H, Schmitt FA (2009): Lewy body pathology in normal elderly subjects. J Neuropathol Exp Neurol 68: 816–822.
83. Błaszczyk JW (2016): Parkinson's disease and neurodegeneration: GABA-collapse hypothesis. Front Neurosci 10:269.
84. Kaur R, Mehan S, Singh S (2019): Understanding multifactorial architecture of Parkinson's disease: Pathophysiology to management. Neurol Sci 40:13–23.
85. Wang J, Wang F, Mai D, Qu S (2020): Molecular mechanisms of glutamate toxicity in Parkinson's disease. Front Neurosci 14:585584.
86. Firbank MJ, Parikh J, Murphy N, Killen A, Allan CL, Collerton D, *et al.* (2018): Reduced occipital GABA in Parkinson disease with visual hallucinations. Neurology 91:e675–e685.
87. Van Nuland AJM, Den Ouden HEM, Zach H, Dirkx MFM, Van Asten JJA, Scheenen TWJ, *et al.* (2020): GABAergic changes in the thalamocortical circuit in Parkinson's disease. Hum Brain Mapp 41:1017–1029.
88. O'Gorman Tuura RL, Baumann CR, Baumann-Vogel H (2018): Beyond dopamine: GABA, glutamate, and the axial symptoms of Parkinson disease. Front Neurol 9:806.
89. Arias de la Torre J, Vilagut G, Ronaldson A, Dregan A, Ricci-Cabello I, Hatch SL, *et al.* (2021): Prevalence and age patterns of depression in the United Kingdom. A population-based study. J Affect Disord 279:164–172.
90. Movement Disorder Society Task Force on Rating Scales for Parkinson's Disease (2003): The Unified Parkinson's Disease Rating Scale (UPDRS): Status and recommendations. Mov Disord 18:738–750.
91. Goetz CG, Poewe W, Rascol O, Sampaio C, Stebbins GT, Counsell C, *et al.* (2004): Movement Disorder Society Task Force report on the Hoehn and Yahr staging scale: Status and recommendations. Mov Disord 19:1020–1028.
92. Fry A, Littlejohns TJ, Sudlow C, Doherty N, Adamska L, Sprosen T, *et al.* (2017): Comparison of sociodemographic and health-related characteristics of UK Biobank participants with those of the general population. Am J Epidemiol 186:1026–1034.
93. Cermakova P, Formanek T, Kagstrom A, Winkler P (2018): Socioeconomic position in childhood and cognitive aging in Europe. Neurology 91:e1602–e1610.
94. Tari B, Künzi M, Pflanz CP, Raymont V, Bauermeister S (2023): Education is power: Preserving cognition in the UK Biobank. Front Public Health 11:1244306.
95. Nikhra V (2017): The aging brain: Recent research and concepts. GGS 1:1.